Received 20 June 2022; revised 23 July 2022; accepted 6 August 2022. Date of publication 10 August 2022; date of current version 19 August 2022.
The review of this article was arranged by Editor Z. Zhang.

Digital Object Identifier 10.1109/JEDS.2022.3197830

Temperature Effect Analysis of the Enzymatic RuO_2 Biomedical Sensor for Ascorbic Acid Detection

PO-YU KUO (Member, IEEE), WEI-HAO LAI, CHUN-HUNG CHANG, AND TAI-HUI WANG

Graduate School of Electronic Engineering, National Yunlin University of Science and Technology, Douliou 64002, Taiwan

CORRESPONDING AUTHOR: P.-Y. KUO (e-mail: kuopy@yuntech.edu.tw)

This work was supported by the Ministry of Science and Technology, Taiwan, under Grant MOST 111-2221-E-224-050 and Grant MOST 110-2221-E-224-051.

ABSTRACT The temperature effect has been discussed in the past on pH sensors. In this study, the temperature effect is analyzed for the ascorbic acid (AA) biosensor based on enzymatic ascorbate oxidase (AO). To reduce this effect, a novel temperature compensation circuit was implemented by Taiwan Semiconductor Manufacturing Co., Ltd. (TSMC) 180 nm complementary metal-oxide-semiconductor (CMOS) process. By applying the proposed circuit, the temperature coefficients (TCs) with five concentrations of AA were suppressed below 201 μV/°C. The TC of the normal level of AA concentration (0.0312 mM) in the human body was 188 μV/°C, at the temperature range from 25°C to 55°C. The polyethylene terephthalate (PET) substrate was utilized. To confirm the stability of the fabricated AO/RuO_2/PET AA biosensor, interference and hysteresis experiments were carried out. At present, the experiments were still in the stage of in vitro measurement. The results showed that the AO/RuO_2/PET AA biosensor had good selectivity that effective against other interference that may exist in blood at either 25 °C or 37.5 °C. Moreover, at the temperature of 37.5 °C, the hysteresis voltage of the biosensor after applying the compensation circuit was reduced from 18.27 mV to 1.39 mV.

INDEX TERMS Temperature effect, temperature compensation circuit, ascorbic acid (AA), ruthenium dioxide (RuO_2), enzymatic biosensor, CMOS process.

I. INTRODUCTION

Temperature influence is one of the important issues for biomedical sensors. Most temperature compensation mechanisms were based on ion-sensitive field-effect transistor (ISFET) sensors [1], [2], [3], [4], [5]. ISFET was first proposed by Bergveld [6]. When the ion concentration (for example, H^+, K^+, Na^+) changes, the current flowing through the transistor also changes accordingly. Furthermore, the metal gate is replaced by an ion-sensitive membrane, electrolyte solution, and reference electrode. Gaddour *et al.* [1] used two ISFETs with the same electrical and chemical characteristics for temperature compensation, called ISFET and reference field effect transistor (ReFET). ReFET sensor can significantly reduce drift and noise of measurement. The feedback of the transconductance amplifier controlled the calibration of the reference electrode to overcome the DC offset and make it easier to achieve differential measurement for the ReFET/ISFET. Chan and Chen [2] proposed a nonlinear temperature compensation method that was based on deriving a unified form for body-effect-based ISFET temperature-dependent threshold voltage. Then repeatedly adjust and correct the bias current of the temperature compensation circuit to make the ISFET work nearby zero temperature coefficient (Z.T.C.). Chin *et al.* [3] proposed a temperature compensation circuit that used a p-n diode of temperature sensor, a constant current constant voltage (CCCV) readout circuits, and an instrumentation amplifier (INA) to perform temperature compensation for a single ISFET. Naimi *et al.* [4] designed the low power consumption ISFET operating in weak and moderate inversion regions based Enz– Krummenacher– Vittoz (EKV) model [7] that describes the ISFET's behavior of temperature. Therefore, they utilized a third-stage read out circuit for this behavior to make the output voltage insensitive to

temperature. Bhardwaj *et al.* [5] introduced electrochemical parameters into the MOSFET model to simulate ISFET behavior. They utilized CCCV readout circuit to read out the voltage signal of ISFET. Smart machine learning based regression models to compensate for the temperature behavior and the output signal of the trained model showed the characteristics independent of temperature. But ISFET has several shortcomings, such as low sensitivity, light influence, poor stability, and the entire device must be remanufactured when the sensing membrane is damaged. To overcome these shortcomings, Spiegel *et al.* [8] proposed the extended gate field effect transistor (EGFET). Fig. 1 illustrated the sensing architecture of EGFET and ISFET. The MOSFET biosensor can operate not only in the saturation region but also in the linear region. The I_{DS}-V_{GS} scanned curves which are obtained from the linear region can convert out the voltage sensitivity and the I_{DS}-V_{DS} scanned curves which are obtained from the saturation region can convert out the current sensitivity. In the configuration of EGFET, the gate of MOSFET is connected to the sensor, and the charge on the sensing film changes due to electrochemical reaction, which affects the conductive condition of the MOSFET. When the sensor is damaged by analytes, we only need to replace the sensing area instead of remanufacturing the entire component. When MOSFET is not operating properly, we can just replace the MOSFET. This feature enables EGFET to successfully overcome the shortcomings of ISFET. Therefore, many researchers have fabricated different metal oxides such as ZnO, CuO, TiO_2, NiO_x, IGZO, and RuO_x [9], [10], [11], [12], [13], [14], as sensors of EGFET for pH detection and glucose detection. However, there is almost no application for ascorbic acid (AA) detection. Batista and Mulato [9] fabricated ZnO thin film by sol-gel method and applied it to EGFET pH detection. Mishra *et al.* [10] grew CuO nanowires on copper foil to detect pH value and glucose. They proved that the threshold voltage changed due to the pH concentration. Li *et al.* [11] utilized an electron beam evaporator to successfully fabricate TiO_2 nanowire and apply it to pH measurement. Pan *et al.* [12] investigated the effect of annealing NiO_x films at different temperatures on silicon substrates for pH sensing. Kim *et al.* [13] developed an IGZO sensing film for EGFET sensor which can detect glucose in tears. Singh *et al.* [14] used the sol-gel method to derive RuO_x thin film as a pH EGFET sensor and found that the RuO_x thin film had a super Nernst sensitivity.

The common name of AA is vitamin C which is one of the vitamins for human body and it cannot be synthesized by the body. AA controls wound healing, collagen synthesizing, skeletal, and tendon [15]. When the concentration of AA in the blood is lower than 0.0078 mM, the lack of AA may cause scurvy. The concentrations of AA over 0.125 mM may cause diarrhea. The most appropriate concentration of AA in the blood should be 0.031 mM [16]. Various methods for AA detection have been developed, such as titration [17], fluorimetric method [18], electrochemistry [19], and enzymatic analysis [20]. Among them, the enzymatic method has

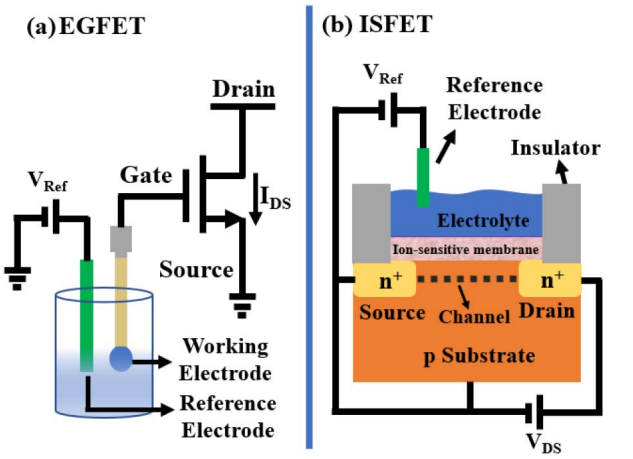

FIGURE 1. Schematic diagram of (a) EGFET and (b) ISFET.

a better reaction rate, sensitivity, selectivity, and accuracy. Hence, we immobilized ascorbate oxidase (AO) on RuO_2 membrane to react with AA.

Ruthenium dioxide (RuO_2) is an oxide that has a rutile structure [21]. It has good metal conductivity, chemical stability, high sensitivity, corrosion resistance, and electrochemical reversibility [14]. It can also be used as a material for supercapacitors [22]. These characteristics enable RuO_2 to act as a working electrode in acidic solutions such as AA. Moreover, the characteristics of supercapacitors make more charge to be stored on the RuO_2 working electrode, resulting in good sensitivity. Many processes for RuO_2 thin films have been developed like sol-gel, magnetron sputtering, atom laser deposition, etc. [14], [23], [24].

Most studies rarely mention the ambient TC of EGFET, and there are almost exclusively based on ISFET studies. In this study, to reduce the temperature effect, we proposed a temperature compensation method for the AO/RuO_2/polyethylene terephthalate (PET) AA biosensor. The previously mentioned temperature compensation circuits were based on pH sensors and the temperature compensation circuit that was proposed in this study is the first applied to biosensors. We utilized two enzymatic RuO_2 AA biosensors with the same electrical properties and manufacturing process to achieve differential measurement which can effectively suppress the temperature impact on the sensor [1], [25], [26]. On the other side, the temperature compensation circuit can intuitively read out the response voltage of the sensor and display its voltage signal through Labview software on the computer. This compensation circuit has the advantages of simple design, easy to use, and effective reduction of the TC for the biosensor.

II. EXPERIMENTAL

The experimental section can be divided into four parts including the use of materials, fabrication process of the AO/RuO_2/PET AA biosensor, reaction mechanism between the enzymatic AO/RuO_2/PET AA biosensor, and

AA solution, and chip design of the temperature compensation circuit.

A. MATERIALS AND EQUIPMENT

The flexible PET as the biosensor substrate was purchased from Zencatec Corporation Co., Ltd. (Taoyuan City, Taiwan), the silver paste as conductive wires were purchased from Advanced Electronic Materials INC. (Tainan City, Taiwan), the RuO_2 target with 99.95% purity was purchased from Ultimate Materials Technology Co., Ltd. (Hsinchu County, Taiwan), the epoxy resin as encapsulation layer was purchased from Sil-More Industrial Co., Ltd. (New Taipei City, Taiwan), the AA powder, AO, 3-Aminopropyltriethoxysilane (γ-APTS), and glutaraldehyde was purchased from Sigma-Aldrich Corp. (St. Louis, MO, USA), the buffer solutions (PBS) of pH 7.0 was purchased from AppliChem GmbH Corp. (Darmstadt, Germany). Many studies are based on PBS to prepare solutions for different analytes [27], [28]. The customized screen-printed machine was purchased from Houn Jien Co., Ltd, (New Taipei City, Taiwan), and the RF sputtering system assembled from various components was purchased from ShiHsin Technology Co., Ltd (Tainan City, Taiwan).

B. FABRICATION OF AO/RUO_2/PET AA BIOSENSOR

To fabricate an enzymatic AO/RuO_2/PET AA biosensor with good quality and stability, we followed the fabrication method of Chou's study [29]. The fabrication process of the AO/RuO_2/PET AA biosensor was illustrated in Fig. 2 [29]. The 3 cm×4 cm of PET substrate was cleaned with acetone, 99% of alcohol, and deionized (DI) water by ultrasonicator for 15 minutes, sequentially. The DI water had a resistivity of 18.4 MΩ.cm. Next, the silver paste was printed on the PET substrate as conductive wires, counter electrode, and reference electrode by screen printing technology. The model of the printing board was a counter electrode, reference electrode, and six arrayed silver conductive wires as working electrodes that were shown in step 1 of Fig. 2. Then the RF sputtering system was used to deposit RuO_2 thin film on the silver layer with RF power of 50 W, process pressure of 10 mTorr, argon to oxygen ratio (Ar : O_2) of 10:1 sccm, and sputtering time of 30 minutes. The sputtering parameters of RuO_2 thin film was shown in Table 1. After depositing the RuO_2 thin film, the epoxy resin was used to encapsulate the exposed silver wires by screen printing technology and baked in an oven at 120 °C for 120 minutes. Then dropped 2 μL of γ-APTS with the concentration of 1 wt% on the RuO_2 film as an adhesive to immobilize AO. γ-APTS had functionalized surfaces. It allowed crosslinking with AO to modify RuO_2 sensing film. The AO of 250 UN was mixed with 200 μL of PBS. When the γ-APTS was dry, dropped 2 μL of AO on the γ-APTS layer as an enzymatic layer. Finally, dropped 2 μL of glutaraldehyde (GA) with the concentration of 1 wt% on the enzymatic AO layer to enhance the adsorption capacity of AO on the RuO_2 sensing film [30].

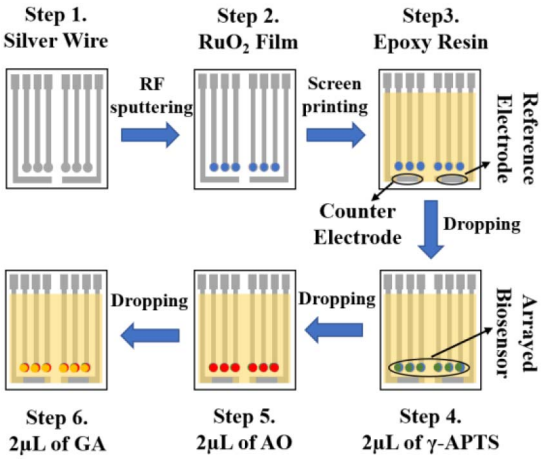

FIGURE 2. The fabrication process of AO/RuO_2/PET AA biosensor [29].

TABLE 1. Sputtering parameters of RUO_2 thin film.

Parameters	Unit
RF Power	50 W
Process Pressure	10 mTorr
Argon to Oxygen Ratio (Ar:O_2)	10:1 sccm
Sputtering Time	30 minutes

C. REACTION MECHANISM BETWEEN THE ENZYMATIC AO/RUO_2/PET AA BIOSENSOR AND AA SOLUTION

The reaction mechanism between the enzymatic AO/RuO_2/PET AA biosensor and AA solution is as follows [31]:

$$L-AA \xrightarrow{AO} Dehydro-L-AA+2H^+ + 2e^- \quad (1)$$

When the AO/RuO_2/PET AA biosensor was immersed in AA solution, AO decompose AA producing dehydrogenated AA, two hydrogen ions, and two electrons. Reversible redox equilibrium exists between two different solid phases/oxidation states of RuO_2 metal oxides [32]. Two hydrogen ions and two electrons which decompose by AO generate potential with the RuO_2 thin film, and the reaction formula is as follows [14]:

$$RuO_2 + nH_2O + H^+ + e^- \longleftrightarrow Ru(OH)_3 + (n-1)H_2O \quad (2)$$

The adsorbed protons attract electrons through the conducting oxide, leading to the reduction of Ru ions. This results in a potential change and causes the measurable change of the potential [33]. The potential of RuO_2 thin film can be as follows [14]:

$$E = E^0 - \frac{RT}{F}\ln\frac{[Ru(OH)_3]}{[RuO_2][H^+]} = \left(E^0 - \frac{RT}{F}\ln\frac{[Ru(OH)_3]}{[RuO_2]}\right) + \frac{RT}{F}\ln[H^+] \quad (3)$$

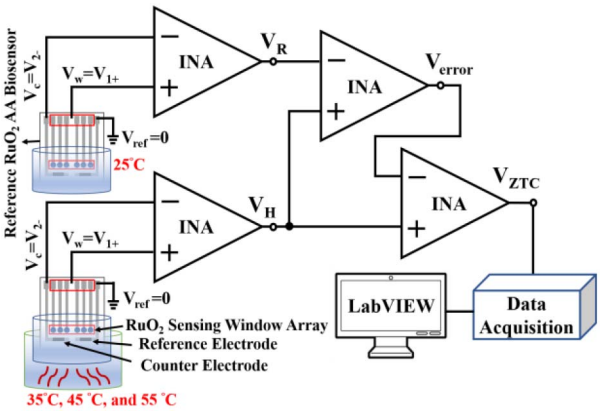

FIGURE 3. The schematic diagram of the proposed temperature compensation circuit.

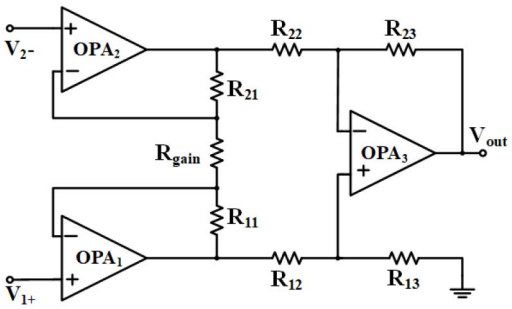

FIGURE 4. The circuit schematic of INA.

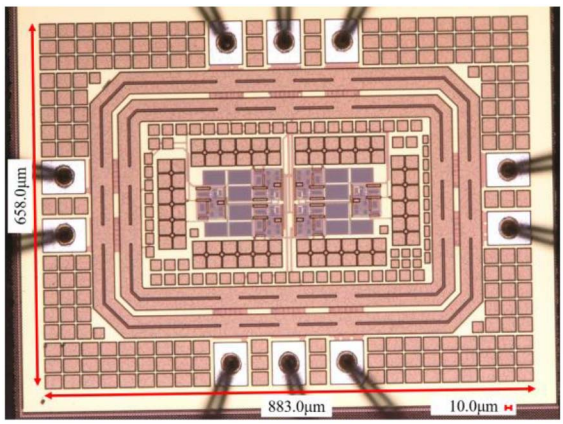

FIGURE 5. The die photo of the temperature compensation circuit.

TABLE 2. Performance of the self-designed INA.

Parameters	Value
Supply Voltage	±1.8 V
Differential mode gain (A_d)	51.32 dB
Common-mode gain (A_{cm})	-69.55 dB
Common-Mode Rejection Ratio (CMRR)	120.87 dB
Offset Voltage	125.78 uV
Input Offset Current	205.50 pA
Power Consumption	1.83 mW

where E^0 is standard electrode potential, R is the universal gas constant, T is absolute temperature, F is Faraday constant, and $[H^+]$, $[RuO_2]$, $[Ru(OH)_3]$ represent the activity of H^+, RuO_2, and $Ru(OH)_3$, respectively. The RuO_2 thin film relies on AO to decompose AA into hydrogen ions. When AO encounters AA, it decomposes hydrogen ions. The concentration of AA is higher, more hydrogen ions were decomposed by AO. According to equation (3), the number of hydrogen ions does change the response voltage of the RuO_2 sensing membrane. Therefore, the hydrogen ions that were generated by AO are used to explain the temperature-dependent behavior of the temperature compensation circuit in the following aspects.

D. VOLTAGE-TIME MEASUREMENT SYSTEM

In this study, the potentiometric biomedical sensing signals were displayed on the computer by the voltage-time (V-T) measurement system as shown in Fig. 3. V_{ZTC} was the temperature-independent output signal of the AO/RuO_2/PET AA biosensor that connected to the data acquisition device (USB-6210, National Instruments, USA). Then, the analog signals of the temperature compensation circuit were converted to digital signals by the data acquisition device. Finally, the data acquisition device transmitted it to the computer. The signals of the AO/RuO_2/PET AA biosensor were displayed on the LabVIEW interface (LabVIEW, National Instruments, USA) of computer.

E. CHIP DESIGN OF TEMPERATURE COMPENSATION CIRCUIT

The proposed temperature compensation circuit was composed of four INAs. To explain the chip design of the temperature compensation circuit, we have first clarified the working principle of the INA and three-electrode system. The circuit diagram of the INA was shown in Fig. 4 and the circuit diagram of the proposed temperature compensation circuit was shown in Fig. 3 which was composed from the INA shown in Fig. 4. All INAs and operational amplifiers (OPAs) were designed by our laboratory and simulated by the electronic design automation (EDA) tool which was provided by Taiwan Semiconductor Research Institute (TSRI). To read out the original biomedical signals, the gain of the INA is set to 1 and the resistance values of R were all designed to be the same as 30 kΩ. During the measurement, R_{gain} was removed to force the gain of the INA was 1. The chip of the temperature compensation circuit was fabricated by Taiwan Semiconductor Manufacturing Co., Ltd. (TSMC) 180 nm complementary metal-oxide-semiconductor (CMOS) process. The die photo of the temperature compensation circuit was shown in Fig. 5. Performances of the self-designed INA were shown in Table 2. This INA had a high common-mode rejection ratio (CMRR) of 120.87 dB. Therefore, the differential input could effectively reduce the influence of noise including

TABLE 3. Comparisons with the commercial INA LT1167.

INA	Supply Voltage (V)	CMRR (dB)	Power Dissipation (mW)
LT1167	2.3 to 18	90	2.07 to 13.5
Proposed INA	1.8	120.87	1.83

temperature. This INA utilized a supply voltage of ±1.8 V and the power consumption was 1.83 mW. The commercial LT1167 is commonly used as a readout circuit for biomedical sensors [34]. Thus, the LT1167 was compared to our proposed INA as shown in Table 3. The proposed INA achieved higher CMRR and lower power consumption, which means better anti-noise capability and power saving. Due to the high input impedance, the low output impedance, and the very low voltage of the biomedical sensor of the proposed INA, the voltage of the biomedical sensor can be completely fed into the next circuit interface.

The INA was constructed from three operational amplifiers. OPA_1 and OPA_2 were the voltage followers which had high input impedance. OPA_3 was the differential amplifier, which was used for differential amplification of two input terminals. The relationship of input signal, resistance, and output signal can be written as follows [35]:

$$\text{Gain} = \frac{V_{out}}{V_{2+} - V_{1-}} = \left(1 + \frac{2R_{21}}{R_{gain}}\right) \times \left(\frac{R_{23}}{R_{22}}\right) \tag{4}$$

The INA performed the subtraction of two voltages from V_{1+} and V_{2-}. The AO/RuO_2/PET AA biosensor utilized a three-electrode system, which were a working electrode, a reference electrode and a counter electrode. V_{1+} was connected to working electrode and V_{2-} was connected to counter electrode and reference electrode was connected to ground. The working principle of three-electrode system can be follows:

$$V_{\text{ref}} = V_{\text{solution}} = 0 \tag{5}$$
$$V_{1+} = V_{\text{w}} - V_{\text{ref}} = V_{\text{w}} \tag{6}$$
$$V_{2-} = V_{\text{c}} - V_{\text{ref}} = V_{\text{c}} \tag{7}$$
$$V_{\text{out}} = V_{1+} - V_{2-} = V_{\text{w}} - -V_{\text{c}} \tag{8}$$

where V_{ref} is voltage of reference electrode, V_{w} is voltage of working electrode, V_{c} is voltage of counter electrode, V_{1+} is positive input of the INA, V_{2-} is negative input of the INA, and V_{out} is output of the INA.

When working electrode, counter electrode, and reference electrode were immersed in solutions, V_{ref} was connected to ground. V_{1+} equal to the potential difference between V_{w} and ground. V_{2-} equal to the potential difference between V_{c} and ground. V_{w} and V_{c} were passively coupled to the input of INA. Working electrode to reference electrode and counter electrode to reference electrode are two differential pairs. Noise immunity can be improved due to the same material of differential pairs [36]. The reference electrode and counter electrode were made of silver. Silver is an inert metal with strong corrosion resistance and provides stable voltage, which can be effectively used as reference electrode and counter electrode by our previous research [30], [37]. V_{out} equal to the voltage of the working electrode minus the voltage of the counter electrode.

Next, the chip design of the temperature compensation circuit is stated. First, we utilized two AO/RuO_2/PET AA biosensors with the same sputtering process which could effectively eliminate the temperature coefficients (TC) of the biosensor [1], [38]. One of the two AO/RuO_2/PET AA biosensors was used as a reference biosensor to give a reference voltage for the compensation circuit and it was kept at room temperature. The other AO/RuO_2/PET AA biosensor was heated in the thermostatic water bath (8402L, FIRSTEK, Taiwan) at 35°C, 45°C, and 55°C. Then, the accurate temperatures were monitored with a commercial thermometer. Five different concentrations of AA, 0.0078 mM, 0.0312 mM, 0.125 mM, 0.5 mM, and 2 mM which were based on PBS solution of pH 7 were measured at each temperature. This range covers the concentrations that cause scurvy (0.0078 mM), the average human body concentration (0.125 mM), and the concentration that is oversaturated (2 mM). The inference of the compensation circuit as shown in Fig. 3 can be follows:

$$\text{V}_{\text{R}} = \left(1 + \frac{2R_{11}}{\infty}\right) \times \left(\frac{R_{13}}{R_{12}}\right) \times \left(V_{W(25°C)} - V_C\right) \tag{9}$$
$$\text{V}_{\text{H}} = \left(1 + \frac{2R_{11}}{\infty}\right) \times \left(\frac{R_{13}}{R_{12}}\right) \times \left(V_{W(T)} - V_C\right) \tag{10}$$

where V_{R} is the reference response voltage of the AO/RuO_2/PET AA biosensor at room temperature, V_{H} is the response voltage of the AO/RuO_2/PET AA biosensor with different temperatures, V_{W} is the response voltage on the AO/RuO_2/PET AA biosensor, ∞is open circuit impedance. The TC of resistance inside INA can be expressed as follows:

$$\text{R} = \text{R}_0 \times [1+\lambda(\text{T} - \text{T}_0)] \tag{11}$$

where R is resistance value at temperature T, R_0 is resistance value at 25°C, λis TC of resistance for different materials, T is the temperature in degrees Celcius, and T_0 is 25°C. Substituting the TC of resistance into formulas (9) and (10). V_{error} can be obtained as follows:

$$\begin{aligned}\text{V}_{error} = &\left(1 + \frac{2R_{11}[1 + \lambda(T - T_0)]}{\infty}\right) \\ &\times \left(\frac{R_{13}[1 + \lambda(T - T_0)]}{R_{12}[1 + \lambda(T - T_0)]}\right) \times \left(V_{W(T)} - V_C\right) \\ &- \left(1 + \frac{2R_{11}[1 + \lambda(T - T_0)]}{\infty}\right) \\ &\times \left(\frac{R_{13}[1 + \lambda(T - T_0)]}{R_{12}[1 + \lambda(T - T_0)]}\right) \times \left(V_{W(25^oC)} - V_C\right)\end{aligned} \tag{12}$$

where V_{error} is error voltage of working electrode caused by the temperature change of the AA solution. The surface potential of V_{w} between the AA solution and RuO_2

TABLE 4. TCS of the AO/RuO_2/PET AA biosensor without and with applying compensation circuit.

Concentrations of AA (mM)	TCs without the Circuit (μV / °C)	TCs with the Circuit (μV / °C)
0.0078	870	89 (Reduce 89.7 %)
0.0312	734	188 (Reduce 74.4 %)
0.1250	289	148 (Reduce 49.0 %)
0.5000	431	181 (Reduce 58.0 %)
2.0000	873	201 (Reduce 77.0 %)

working electrode can be written according to the Nernst equation [14]:

$$V_w = E^0 - \frac{RT}{F} \ln \frac{[Ru(OH)_3]}{[RuO_2][H^+]} \tag{13}$$

From the formula (13), the potential of RuO_2 thin film was related to temperature T. The ions were distributed only between the AA solutions and the surface of the working electrode, with neither electron nor ion exchange at the two-phase boundary [39]. Then subtract V_{error} of formula (12) from V_H of formula (10) to get V_{ZTC} which is the output voltage independent of temperature. V_{ZTC} can be written as follows:

$$\begin{aligned} V_{ZTC} = &\left(1 + \frac{2R_{11}[1 + \lambda(T - T_0)]}{\infty}\right) \\ &\times \left(\frac{R_{13}[1 + \lambda(T - T_0)]}{R_{12}[1 + \lambda(T - T_0)]}\right) \\ &\times \left(\left(E^0 - \frac{RT}{F} \ln \frac{[Ru(OH)_3]}{[RuO_2][H^+]}\right) - V_C\right) - (V_{error}) \end{aligned} \tag{14}$$

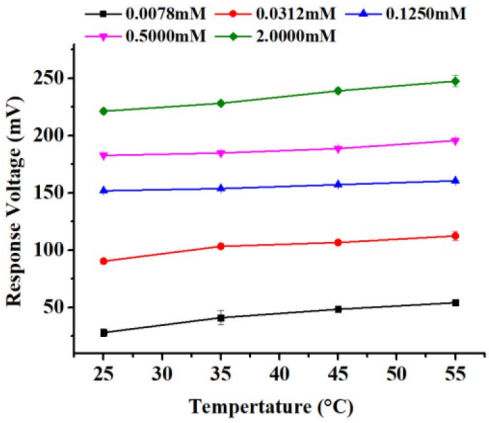

FIGURE 6. The response voltage at different temperatures without compensation circuit.

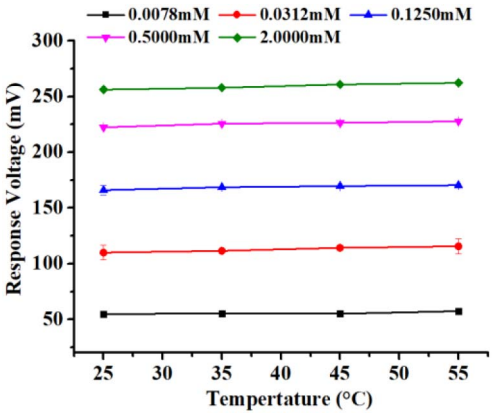

FIGURE 7. The response voltage at different temperatures with applying compensation circuit.

III. RESULTS AND DISCUSSION

A. TEMPERATURE COEFFICIENT OF THE AO/RUO_2/PET AA BIOSENSOR WITHOUT AND WITH THE COMPENSATION

In the five concentrations of AA from 0.0078 mM to 2 mM, the AO/RuO_2/PET AA biosensor had different TCs according to the equation (13). In this study, the temperature range was set as 25°C, 35°C, 45°C, and 55°C. The actual TC measurement results of the AO/RuO_2/PET AA biosensor without and with applying the compensation circuit were shown in Fig. 6 and Fig. 7. Those data of TCs before and after applying the compensation circuit were presented in Table 4. At the 0.0078 mM AA, there is the lowest TC of 89 μV/°C. With compensation, this TC of 0.0078 mM AA is reduced by about 89%. The five TCs can be effectively reduced by more than 49% (At 0.125 mM AA) with temperature compensation. The compensation results are valid because no matter what the AA concentration is, at least 49% of the TC is inhibited. According to Fig. 6, the response voltage of the AO/RuO_2/PET AA biosensor significantly increased with the increase in temperature. At 55°C, the response voltage of the AO/RuO_2/PET AA biosensor had apparent voltage changes. With the temperature compensation circuit, the response voltage which was shown in Fig. 7 was flat in the case of temperature rise. Different concentrations of AA corresponding to response voltage at different temperatures were described in Fig. 8. The response voltage of the AO/RuO_2/PET AA biosensor was obviously close to the response voltage at 25 °C whether the AO/RuO_2/PET AA biosensor was operated at 35°C, 45°C, or 55°C. The dependence of the AO/RuO_2/PET AA biosensor on temperature was effectively reduced through the proposed circuit. It can be seen that no matter how the temperature changed, the response voltage with different concentrations of AA were superimposed on 25°C. Thus, the response voltages of 35°C, 45°C, and 55°C, were corrected to the voltage at 25°C.

B. INTERFERENCE EXPERIMENT OF THE AO/RUO_2/PET AA BIOSENSOR BASED ON BODY TEMPERATURE

To make sure the AO/RuO_2/PET AA biosensor suitable for measurement of human blood, the PBS solution of pH 7, AA of 0.125 mM, lactic acid (LA) of 0.8 mM, glucose (GLC) of 5 mM, urea (UR) of 5 mM, uric acid (UA) of 0.3 mM, dopamine (DA) of 0.06 mM, and AA of 2 mM were heated to 37.5°C by a thermostatic water bath. The

TABLE 5. Comparative study of temperature compensation methods and TCS.

Analytes	Process	Power Supply	Temperature Ranges	TC	References
pH 6	TSMC (0.18 μm)	1.8 V	0°C – 50°C	0.005 mV/°C	2020 [1]
pH 12	MOSIS (AMI 1.0 μm)	3.0 V	20°C – 60°C	0.028 mV/°C	2014 [4]
pH 6	TSMC (0.35 μm)	1.65 V	5°C – 35°C	0.320 mV/°C	2016 [40]
pH 7	N/A	N/A	24˚C– 70˚C	0.295 mV/°C	2016 [42]
0.0312 mM of AA	TSMC (0.18 μm)	1.8 V	25˚C – 55˚C	0.188 mV/°C	This study

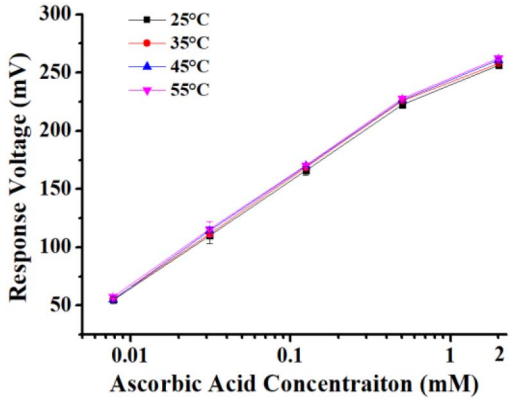

FIGURE 8. The response voltage at different temperatures with the temperature compensation circuit.

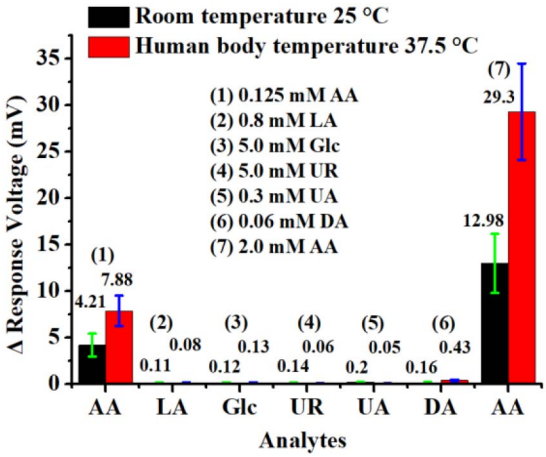

FIGURE 9. Interference experiment of the AO/RuO_2/PET AA biosensor at 25°C and 37.5°C.

interference experiments of the AO/RuO_2/PET AA biosensor were carried out at 25°C and 37.5°C, respectively. The concentrations of these interfering substances were within the range of human blood [41]. First, soak the AO/RuO_2/PET AA biosensor in a blank PBS solution until the response voltage of the AO/RuO_2/PET AA biosensor was stable. Then, added 200 μL of AA solutions and interfering substances in the blank PBS solution in order as shown in Fig. 9. The interference experiment of the AO/RuO_2/PET AA biosensor at 25°C and 37.5°C were shown in Fig. 9. The histograms were illustrated by calculating the amount of response voltage changed after adding those substances. This experiment was performed without a temperature compensation circuit. The temperature of 37.5°C enhanced the activity of AO. Thus, by adding 0.125 mM AA and 2 mM AA to the blank PBS solution, the response voltage of the AO/RuO_2/PET AA biosensor changed about double due to the temperature. By adding 0.125 mM AA to the blank PBS solution, the change of response voltage was 4.21 mV at 25°C. By adding 2.0 mM AA to the blank PBS solution, the change of response voltage was 12.98 mV at 25°C. When other interferents were added, the change of response voltage was almost unaffected (less than 0.5 mV). This can explain that the AO/RuO_2/PET AA biosensor can generate a corresponding response voltage after encountering AA, and other interfering substances do not affect the response voltage. Thus, the AO/RuO_2/PET AA biosensor has good specificity for AA. This can be attributed to the good selectivity of the AO/RuO_2/PET AA biosensor after the modification of AO which was possible to realize the ideal ReFET, and other interfering substances had little effect to the response voltage of the AO/RuO_2/PET AA biosensor.

Table 5 showed the comparative study of temperature compensations. Gaddour *et al.* [1] utilized two ISFETs with the same process for temperature compensation through differential measurement and designed operational transconductance amplifiers (OTAs) as an instrumentation amplifier to immune temperature interference. Naimi *et al.* [4] analyzed ISFET sensor operating in a weakly and moderately inversion states, and a simplified version of the EKV model of the site-binding model describes the behavior of ISFET in response to changes in temperature. According to this model, they designed a readout circuit with high thermal stability to suppress temperature effect. Chung *et al.* [40] used differential measurement to reduce drift, body effect, and temperature effect. Since the compensation circuit was integrated with the ISFET, the on-chip sensing film was damaged by solutions, and the entire ISFET and compensation circuit components need to be re-manufactured. Yusof *et al.* [42] investigated the temperature effect of TiO_2 thin film applied to EGFET sensor. The experimental results showed that the temperature dependence of ISFET is much larger than that of EGFET. Our proposed compensation circuit and biosensor were two separate components. When the biosensor was exhausted, the biosensor can be replaced immediately based on the separate biosensor, and also the part of the temperature compensation circuit can be retained.

C. HYSTERESIS EFFECT UNDER TEMPERATURE EFFECT OF THE AO/RUO_2/PET AA BIOSENSOR

Hysteresis effect is a non-ideal effect and it cannot be avoided [43]. The hysteresis voltage was generated because the rate of diffusion of H^+ ions to the buried sites of the sensing membrane varies with different concentrations of AA [44]. Hysteresis is often present in conducting metal oxides, depending on various factors, such as different oxidation states, internal defects, and diffusing ions. It is related to the chemical interaction between ions in the electrolyte and the slow-reacting surface sites below the membrane surface and the surface defects of the membrane [14], [45]. The experiment of hysteresis effect at 37.5°C confirms whether the AO/RuO_2/PET AA biosensor was corrected to the hysteresis voltage as room temperature through the temperature compensation circuit when the AO/RuO_2/PET AA biosensor was immersed in a AA concentration cycle of 0.03125 mM→0.0078 mM→0.03125 mM→0.125 mM→ 0.03125 mM. Hysteresis effect of the AO/RuO_2/PET AA biosensor at 37.5°C was shown in Fig. 10. The recording time of hysteresis effect lasted 300 seconds. The AO/RuO_2/PET AA biosensor was soaked in each concentration of AA for 60 seconds, and the response voltages for each second were recorded in Fig. 10. Hysteresis effect with temperature which was higher than room temperature was shown as the black line. The initial concentration of 0.03125 mM AA can be attributed to AO reacting more violently at a higher temperature, so the response voltage changed significantly. The enzyme activity gradually stabilized after soaking the sensor for some time. Therefore, the response voltage becomes more stable. The response voltages were measured with and without a compensation circuit for the same period. With the compensation circuit, the response voltage generated by the site binding model of the heated sensor (V_H) can be corrected to the site binding situation at 25°C which means V_{ZTC}. The hysteresis voltage without the compensation circuit was 18.27 mV and the hysteresis voltage with the compensation circuit was 1.39 mV. The hysteresis voltages were obtained by taking the average response voltage of the first concentration (0.03125mM) minus the average response voltage of the last concentration (0.03125mM). In this study, the proposed circuit was first applied to the temperature compensation for AA detection which was based on the enzymatic biomedical sensor. The above researches were applied to temperature compensation of the non-enzymatic pH sensor. Since the activity of the enzyme decreased due to time or temperature, the TCs of enzymatic biosensors were larger than pH sensors. However, through the proposed temperature compensation circuit, the TCs could be controlled below 200 μV/°C within five concentrations of AA. In the future, it is hoped that Ringer's solution or the simulated body fluid can be used to replace the PBS solution. Moreover, the temperature compensation circuit can also be widely applied to other biosensors of different analytes, such as urea, uric acid, glucose, and dopamine.

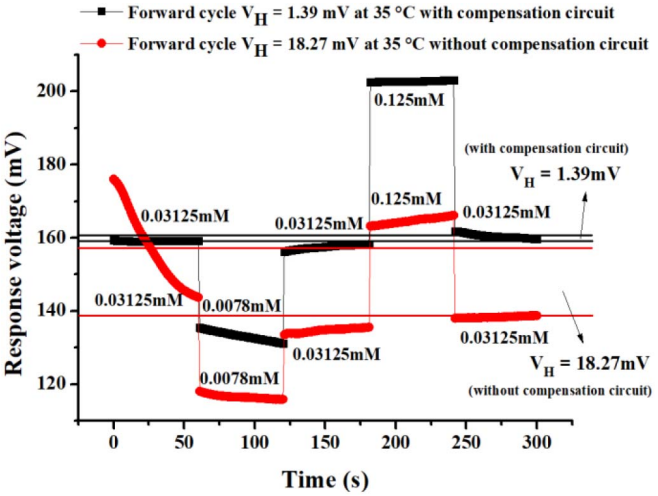

FIGURE 10. Hysteresis effect of the AO/RuO_2/PET AA biosensor at 37.5°C with temperature compensation.

IV. CONCLUSION

This study proposed a novel temperature compensation circuit using 180 nm CMOS process that was applied to the AO/RuO_2/PET AA biosensor. In the temperature range from 25°C to 55°C, the TC for AA of 0.0312 mM was suppressed from 734 μV/°C to 188 μV/°C. The TCs with five concentrations of AA were suppressed at least twice as compared before and after applying the compensation circuit by the compensation circuit. The hysteresis voltage can also be effectively reduced by the temperature compensation circuit. The hysteresis voltage at 37.5°C was 18.27 mV without the compensation circuit. After applying the compensation circuit, the hysteresis voltage was reduced to 1.39 mV. Moreover, the fabricated AO/RuO_2/PET AA biosensor had the good capability of anti-interference. The response voltage was barely affected by the interference substances that may exist in human blood. It can be expected that the proposed temperature compensation circuit will be applied to a wide range of other biosensors in the future.

ACKNOWLEDGMENT

The authors would like to extend their appreciation to the Taiwan Semiconductor Research Institute (TSRI) for the technical support they most generously extended.

REFERENCES

[1] A. Gaddour, W. Dghais, B. Hamdi, and M. B. Ali, "Temperature compensation circuit for ISFET sensor," *J. Low Power Electron. Appl.*, vol. 10, no. 1, p. 2, Jan. 2020.
[2] P. K. Chan and D. Y. Chen, "A CMOS ISFET interface circuit with dynamic current temperature compensation technique," *IEEE Trans. Circuits Syst. I, Reg. Papers*, vol. 54, no. 1, pp. 119–129, Jan. 2007.
[3] Y.-L. Chin, J.-C. Chou, T.-P. Sun, W.-Y. Chung, and S.-K. Hsiung, "A novel pH sensitive ISFET with on chip temperature sensing using CMOS standard process," *Sens. Actuat. B, Chem.*, vol. 76, nos. 1–3, pp. 582–593, Apr. 2001.
[4] S. E. Naimi, B. Hajji, I. Humenyuk, J. Launay, and P. Temple-Boyer, "Temperature influence on pH-ISFET sensor operating in weak and moderate inversion regime: Model and circuitry," *Sens. Actuat. B, Chem.*, vol. 202, pp. 1019–1027, Oct. 2014.

[5] R. Bhardwaj, S. Sinha, N. Sahu, S. Majumder, P. Narang, and R. Mukhiya, "Modeling and simulation of temperature drift for ISFET-based pH sensor and its compensation through machine learning techniques," *Int. J. Circuit Theory Appl.*, vol. 47, no. 6, pp. 954–970, Mar. 2019.

[6] P. Bergveld, "Development of an ion-sensitive solid-state device for neurophysiological measurements," *IEEE Trans. Biomed. Eng.*, vol. BME-17, no. 1, pp. 70–71, Jan. 1970.

[7] C. C. Enz, F. Krummenacher, and E. A. Vittoz, "An analytical MOS transistor model valid in all regions of operation and dedicated to low-voltage and low-current applications," *Analog Integr. Circuits Signal Process.*, vol. 8, no. 1, pp. 83–114, Oct. 1995.

[8] J. Van Der Spiegel, I. Lauks, P. Chan, and D. Babic, "The extended gate chemically sensitive field effect transistor as multi-species microprobe," *Sens. Actuat.*, vol. 4, pp. 291–298, Jan. 1983.

[9] P. Batista and M. Mulato, "ZnO extended-gate field-effect transistors as pH sensors," *Appl. Phys. Lett.*, vol. 87, no. 14, Sep. 2005, Art. no. 143508.

[10] A. K. Mishra, D. K. Jarwal, B. Mukherjee, A. Kumar, S. Ratan, and S. Jit, "CuO nanowire-based extended-gate field-effect-transistor (FET) for pH sensing and enzyme-free/receptor-free glucose sensing applications," *IEEE Sensors J.*, vol. 20, no. 9, pp. 5039–5047, May 2020.

[11] J. Y. Li, S. P. Chang, S. J. Chang, and T. Y. Tsai, "Sensitivity of EGFET pH sensors with TiO_2 nanowires," *ECS Solid-State Lett.*, vol. 3, no. 10, pp. 123–126, Aug. 2014.

[12] T.-M. Pan, C.-H. Lin, and S.-T. Pang, "Structural and sensing characteristics of NiO_x sensing films for extended-gate field-effect transistor pH sensors," *IEEE Sensors J.*, vol. 21, no. 3, pp. 2597–2603, Feb. 2021.

[13] H. Kim, Y. S. Rim, and J.-Y. Kwon, "Evaluation of metal oxide thin-film electrolyte-gated field effect transistors for glucose monitoring in small volume of body analytes," *IEEE Sensors J.*, vol. 20, no. 16, pp. 9004–9010, Aug. 2020.

[14] K. Singh, B. S. Lou, J. L. Her, S. T. Pang, and T. M. Pan, "Super nernstian pH response and enzyme-free detection of glucose using sol-gel derived RuO_x on PET flexible-based extended-gate field-effect transistor," *Sens. Actuat. B, Chem.*, vol. 298, Nov. 2019, Art. no. 126837.

[15] G.-H. Wu, Y.-F. Wu, X.-W. Liu, M.-C. Rong, X.-M. Chen, and X. Chen, "An electrochemical ascorbic acid sensor based on palladium nanoparticles supported on graphene oxide," *Analytica Chimica Acta*, vol. 745, pp. 33–37, Oct. 2012.

[16] M. Noroozifar, M. Khorasani-Motlagh, R. Akbari, and M. B. Parizi, "Simultaneous voltammetric measurement of ascorbic acid, epinephrine, uric acid and tyrosine at a glassy carbon electrode modified with nanozeolite-multiwall carbon nanotube," *Anal. Bioanal. Chem. Res.*, vol. 1, pp. 62–72, Jun. 2014.

[17] L. Suntomsuk, W. Gritsanapun, S. Nilkamhank, and A. Paochom, "Quantitation of vitamin C content in herbal juice using direct titration," *J. Pharm. Biomed. Anal.*, vol. 28, pp. 849–855, Jun. 2002.

[18] X. Wu, Y. Diao, C. Sun, J. Yang, Y. Wang, and S. Sun, "Fluorimetric determination of ascorbic acid with o-phenylenediamine," *Talanta*, vol. 53, pp. 95–99, Jan. 2003.

[19] J.-M. Zen, D.-M. Tsai, A. S. Kumar, and V. Dharuman, "Amperometric determination of ascorbic acid at a ferricyanide-doped tosflex-modified electrode," *Electrochem. Commun.*, vol. 2, pp. 782–785, Nov. 2000.

[20] N. B. Saari, A. Osman, J. Selamat, and S. Fujita, "Ascorbate oxidase from starfruit (averrhoa carambola): Preparation and its application in the determination of ascorbic acid from fruit juices," *Food Chem.*, vol. 66, no. 1, pp. 57–61, Jul. 1999.

[21] J. H. Huang and J. S. Chen, "Material characteristics and electrical property of reactively sputtered RuO_2 thin films," *Thin Solid Films*, vol. 382, nos. 1–2, pp. 139–145, Feb. 2001.

[22] K.-H. Chang, C.-C. Hu, and C.-Y. Chou, "Textural and pseudocapacitive characteristics of Sol–Gel derived $RuO_2 \cdot xH_2O$: Hydrothermal annealing vs. annealing in air," *Electrochimica Acta*, vol. 54, no. 3, pp. 978–983, Jan. 2009.

[23] B. Xu and W.-D. Zhang, "Modification of vertically aligned carbon nanotubes with RuO_2 for a solid-state pH sensor," *Electrochimica Acta*, vol. 55, no. 8, pp. 2859–2864, Mar. 2010.

[24] J. H. Kim, J. H. Ahn, S. W. Kang, J. S. Roh, S. H. Kwon, and J. Y. Kim, "Thermal stability of RuO_2 thin films prepared by modified atomic layer deposition," *Current Appl. Phys.*, vol. 12, pp. S160–S163, Sep. 2012.

[25] J.-F. Cheng, J.-C. Chou, T.-P. Sun, S.-K. Hsiung, and H.-L. Kao, "New calibration methods to eliminate the non-ideal effect of drift and hysteresis in all-solid-state potassium electrode," *IEEE Sensors J.*, vol. 11, no. 5, pp. 1263–1273, May 2011.

[26] H. J. N. P. D. Mello, and M. Mulato, "Well-established materials in microelectronic devices systems for differential-mode extended-gate field effect transistor chemical sensors," *Microelectron. Eng.*, vol. 160, pp. 73–80, Jul. 2016.

[27] J.-C. Chen, J.-C. Chou, T.-P. Sun, and S.-K. Hsiung, "Portable urea biosensor based on the extended-gate field effect transistor," *Sens. Actuat. B, Chem.*, vol. 91, nos. 1–3, pp. 180–186, Jun. 2003.

[28] L. Zhang *et al.*, "Highly selective and sensitive sensor based on an organic electrochemical transistor for the detection of ascorbic acid," *Biosens. Bioelectron.*, vol. 100, pp. 235–241, Feb. 2018.

[29] J.-C. Chou *et al.*, "Flexible arrayed enzymatic L-ascorbic acid biosensor based on IGZO/Al membrane modified by graphene oxide," *IEEE Trans. Nanotechnol.*, vol. 17, no. 3, pp. 452–459, May 2018.

[30] Y.-H. Nien *et al.*, "Investigation of flexible arrayed urea biosensor based on graphene oxide/nickel oxide films modified by Au nanoparticles," *IEEE Trans. Instrum. Meas.*, vol. 70, pp. 1–9, Aug. 2021.

[31] H. Wang and S. Mu, "Bioelectrochemical response of the polyaniline ascorbate oxidase electrode," *J. Electroanal. Chem.*, vol. 436, nos. 1–2, pp. 43–48, Oct. 1997.

[32] E. Tanumihardja, W. Olthuis, and A. Van den Berg, "Ruthenium oxide nanorods as potentiometric pH sensor for organs-on-chip purposes," *Sensors*, vol. 18, no. 9, p. 2901, Sep. 2018.

[33] P. Kurzweil, "Metal oxides and ion-exchanging surfaces as pH sensors in liquids: State-of-the-art and outlook," *Sensors*, vol. 9, no. 6, pp. 4955–4985, Jun. 2009.

[34] S. A. Pullano *et al.*, "EGFET-based sensors for bioanalytical applications: A review," *Sensors*, vol. 18, no. 11, pp. 4042–4065, 2018.

[35] S. J. Azhari and H. Fazlalipoor, "CMRR in voltage-op-amp-based current-mode instrumentation amplifiers (CMIA)," *IEEE Trans. Instrum. Meas.*, vol. 58, no. 3, pp. 563–569, Mar. 2009.

[36] P.-Y. Kuo and Y.-Y. Chen, "A novel low unity-gain frequency and low power consumption instrumentation amplifier design for RuO2 uric acid biosensor measurement," *IEEE Trans. Instrum. Meas.*, vol. 70, pp. 1–9, Feb. 2021.

[37] J.-C. Chou *et al.*, "Improving the properties of L-ascorbic acid biosensor based on GO/IGZO/Al using magnetic beads," *IEEE Trans. Electron Devices*, vol. 66, no. 4, pp. 1924–1929, Apr. 2019.

[38] N. Mokhtarifar, F. Goldschmidtboeing, and P. Woias, "Low-cost EGFET-based pH-sensor using encapsulated ITO/PET-electrodes," in *Proc. IEEE Int. Instrum. Meas. Technol. Conf. (I2MTC)*, Jul. 2018, pp. 1–5.

[39] C. D. Fung, P. W. Cheung, and W. H. Ko, "A generalized theory of an electrolyte-insulator-semiconductor field-effect transistor," *IEEE Trans. Electron Devices*, vol. 33, no. 1, pp. 8–18, Jan. 1986.

[40] W.-Y. Chung, C.-H. Yang, D. G. Pijanowska, P. B. Grabiec, and W. Torbicz, "ISFET performance enhancement by using the improved circuit techniques," *Sens. Actuat. B, Chem.*, vol. 113, no. 1, pp. 555–562, Jan. 2006.

[41] J.-C. Chou, R.-T. Chen, Y.-H. Liao, J.-S. Chen, M.-S. Huang, and H.-T. Chou, "Dynamic and wireless sensing measurements of potentiometric glucose biosensor based on graphene and magnetic beads," *IEEE Sensors J.*, vol. 15, no. 10, pp. 5718–5725, Oct. 2015.

[42] K. A. Yusof, R. A. Rahman, M. A. Zulkefle, S. H. Herman, and W. F. H. Abdullah, "EGFET pH sensor performance dependence on sputtered TiO_2 sensing membrane deposition temperature," *J. Sens.*, vol. 2016, pp. 1–10, Aug. 2016. [Online]. Available: https://www.hindawi.com/journals/js/2016/7594531/

[43] A. Das *et al.*, "Highly sensitive palladium oxide thin film extended gate FETs as pH sensor," *Sens. Actuat. B, Chem.*, vol. 205, pp. 199–205, Dec. 2014.

[44] P.-C. Yao, J.-L. Chiang, and M.-C. Lee, "Application of sol–gel TiO_2 film for an extended-gate H^+ ion-sensitive field-effect transistor," *Solid-State Sci.*, vol. 28, pp. 47–54, Feb. 2014.

[45] S. Palit, K. Singh, B.-S. Lou, J.-L. Her, S.-T. Pang, and T.-M. Pan, "Ultrasensitive dopamine detection of indium-zinc oxide on PET flexible based extended-gate field-effect transistor," *Sens. Actuat. B, Chem.*, vol. 310, pp. 127850–127858, May 2020.